Acta Materialia 222 (2022) 117417

Contents lists available at ScienceDirect

Acta Materialia

journal homepage: www.elsevier.com/locate/actamat

Full length article

Revealing the structural role of MgO in aluminosilicate glasses

Binghui Deng[a,*], Ying Shi[b], Qi Zhou[c], Mathieu Bauchy[c]

[a] Manufacturing Technology & Engineering, Corning Incorporated, Corning, NY 14831, USA
[b] Science & Technology, Corning Incorporated, Corning, NY 14831, USA
[c] Department of Civil and Environmental Engineering, University of California, Los Angeles, CA 90095, USA

ARTICLE INFO

Article history:
Received 9 August 2021
Revised 2 October 2021
Accepted 14 October 2021
Available online 25 October 2021

Keywords:
Glass intermediate
Ring structure
Network former
Network modifier
MgO

ABSTRACT

The addition of MgO to aluminosilicate glasses usually leads to significant changes for many macroscopic properties. The underlying microscopic structure origin of this effect, however, remains elusive. We herein conduct systematic studies to reveal the structural role of MgO in sodium aluminosilicate glasses over a wide composition range from peralkaline to peraluminous using molecular dynamics simulations. Our results provide pieces of evidence to show that MgO plays a dual role of glass network modifier/charge compensator and network former, with the balance of these two roles strongly depending on the composition of other oxides in the glass. Specifically, Mg^{2+} tends to play a network modifier/charge compensator role when the glass simultaneously contains large amount Al atoms that need to charge balanced and a low concentration of other modifier oxides. In contrast, Mg^{2+} exhibits a more pronounced network-forming role in Al-poor glasses. Additionally, by considering the structural role of MgO in the glass network, we further demonstrate that the non-linear evolution of the isokom annealing temperature upon increasing Al_2O_3 content in the peraluminous regime can be rationalized in terms of the combined effects of short-range connectivity and medium-range ring size distribution. The findings provide insights to further exploit MgO in making glasses with advanced properties.

1. Introduction

Alkali and alkaline earth aluminosilicate glasses have faced great success in many industrial and technological applications, such as chemically strengthened Corning® Gorilla® glass [1,2], liquid crystal display substrates [3,4], and nuclear waste storage [5,6]. Al_2O_3 has been playing an influencing role in these glasses because it offers significant improvement regarding many desirable glass performances, such as chemical durability, mechanical properties, and various other thermodynamics behaviors [7–10]. One of the key factors is that Al_2O_3 can effectively control the degree of glass network polymerization by "consuming" non-bridging oxygen, that is, by transforming network modifiers (e.g., alkali oxides) into charge compensators. Details on the local coordination environment of Al atoms and how it is affected by composition and other processing conditions have been extensively reported in many studies over the past few decades, both by experiments [11–20] and atomistic simulations [10, 21-24].

Even though the effect of alkali oxides on the structure of aluminosilicate glasses is fairly well understood [10,13,21], the effect of alkaline earth oxides turns out to be more complicated, particularly for glasses containing notable amount of MgO. Compared with Ca^{2+}, Mg^{2+} has a strong field strength due to its relatively small radius, thus leading to low coordination number (CN) of 4.5-to-5 as compared to the high CN of 6 for Ca^{2+} [25,26]. However, Mg^{2+} and Zn^{2+} share similar ionic radius and field strength, thus the impact of Mg^{2+} on aluminosilicate glass structure and properties is similar to that of Zn^{2+} as demonstrated by Smedskjaer *et al.* in an outstanding work [27]. Historically, MgO has been considered as a glass network modifier by Zachariasen [28] (since MgO cannot form a glass on its own and violate the four rules of glass formation) and by Sun [29] (based on its single bond energy criterion), or as an intermediate species by Dietzel [30] (based on its cation field strength).

Recently, many studies have suggested that the role of Mg^{2+} lies in between the traditional network modifier and network former roles, i.e., that Mg^{2+} acts as an intermediate species. For instance, Eckert *et al.* [31] have shown that Mg^{2+} plays a partial network former role in a high crack-resistant $60SiO_2$-$10Al_2O_3$-$10B_2O_3$-$10MgO$-$10Na_2O$ glasses by detailed NMR study. Mauro and Smedskjaer *et al.* [32] studied the composition-structure-property relationships in 20 sodium aluminosilicate glasses with MgO-for-CaO substitution, and suggested that the widely observed glass property difference might be attributed to the fact that Mg competes with Al and Si in network-forming positions and is not entirely

* Corresponding author.
E-mail address: dengb@corning.com (B. Deng).

https://doi.org/10.1016/j.actamat.2021.117417
1359-6454/

available for modifying the glass network or charge-balancing Al^{IV} atoms. Moreover, Lee *et al.* [33] and Bechgaard *et al.* [34] have shown that MgO can help to violate the Al-avoidance in aluminosilicate glasses by careful NMR study and Raman spectroscopy study, respectively. Interestingly, Souza *et al.* [35], on the other hand, have suggested that MgO does not act as a network intermediate but simply as a network modifier in a series of bioactive glasses with the compositions of $24.3Na_2O$–$26.9(xCaO$–$(1-x)MgO)$–$46.3SiO_2$–$2.5P_2O_5$ (x = 1, 0.875, 0.75, 0.625 and 0.5) by NMR study. Even within the composition space of aluminosilicate glasses, the role of MgO also remains debated. The apparent contradiction between all these conflicting reports can be resolved by considering that the structure role of MgO depends on the glass composition.

However, revealing how composition governs the role played by Mg^{2+} has thus far been limited by a lack of knowledge regarding their local structure at different length scales. Specifically, although the short-range order of Mg has been investigated (e.g., in terms of bond length, coordination number, etc.) [34,36], little is known regarding the effect of Mg on the ring structure of glasses because of lack of effective experimental approaches to directly probe the structure at that length scale. Atomistic simulations are capable of easily accessing the medium-range structure, even though glasses generated by these approaches tend to be more disordered than their experimental counterparts due to the much higher cooling rate used in simulations [37]. However, insights obtained from simulations with respect to short- and medium-range structures on many glass systems have proven to be useful to reveal structural details that are challenging to access experimentally [10,12, 38-42].

To explore the structural role of MgO in aluminosilicate glasses, we herein carry out a combination of neutron total scattering measurements and molecular dynamics (MD) simulations of a series of sodium aluminosilicate glasses that have been well studied by Mauro and Smedskjaer *et al.* [8,32,34,43] for many other aspects. By taking advantage of ring size distribution and coordination number analysis, our study provides direct evidence to show that Mg^{2+} indeed participates in the glass network formation—wherein the degree of participation largely depends on the composition of the glass.

2. Experimental and simulation methods

2.1. Experiment sample preparation

The nominal compositions (mol%) of the glasses under study are (76 - x)SiO_2–xAl_2O_3–$16Na_2O$–8MgO with x = 0, 2.7, 5.3, 8, 10.7, 13.3, 16, 18.7, 21.3, and 24. The compositions range widely from peralkaline to peraluminous, which is believed to be a good choice for studying the structure role of MgO. If some Mg^{2+} cations enter the glass network by forming MgO_4 tetrahedron in the same way as AlO_4 tetrahedron, Mg^{2+} and Al^{3+} will have to compete for the Na^+ cations for charge compensation, thus the structure role of MgO will be clearly revealed by analyzing its local structure configuration change with varying Si/Al ratio. These glasses have been synthesized and thoroughly studied with respect to various properties by Mauro and Smedskjaer *et al.* in previous studies [8,32,34,43]. Readers are encouraged to check out the detailed melting and quenching procedures for these glasses from those studies. For convenience, we also tabulate the real compositions for these 10 glasses in the Supplementary Material. In this study, we probe the structure role of MgO in these glasses, particularly the medium-range structure, by taking advantage of analyzing the first sharp diffraction peak (FSDP) of total neutron scattering structure factor.

2.2. Neutron scattering measurement

We take the time-of-flight (TOF) neutron total scattering measurements on the Nanoscale-Ordered Materials Diffractometer (NOMAD) at the Spallation Neutron Source (SNS), Oak Ridge National Laboratory [44]. Powdered samples (~200 mg) are loaded into a fused quartz capillary (3 mm diameter), and a data acquisition time of ~30 min is used, achieving a total proton charge of 1.8×10^{12} [45]. Neutron total scattering structure functions are processed using the IDL software developed for the NOMAD instrument [44]. All the structure factors used in this study are normalized to absolute scale utilizing the low-r of G(r) criterion as described in Ref. [46]. The main motivation for performing neutron scattering measurement rather than the commonly used X-ray scattering technique is that ring size distribution can only be reliably decoded from the shape of FSDP of the neutron total scattering structure factor [45]. More specifically, the structure factor of fused silica from neutron scattering contains a well-defined FSDP and principle peak (2^{nd} peak), while the FSDP is much broader and the 2^{nd} peak is missing from the X-ray scattering structure factor [45].

2.3. RingFSDP

To experimentally access the ring size distribution for these glasses, we take advantage of our latest developed and validated RingFSDP method [45,47]. Specifically, the RingFSDP method offers an empirical approach to deconvolve the FSDP of neutron total scattering structure factor into three Gaussian distributions with fixed average reciprocal lengths Q, wherein each distribution is ascribed to a certain family of rings: (i) large rings ($\geq$ 6-membered) centered at low Q, (ii) medium rings (5-membered) centered at intermediate Q, and (iii) small rings ($\leq$ 4-membered) centered at high Q [45]. The population of each ring type is estimated to be proportional to the relative integrated area under each Gaussian distribution. Therefore, the ring size distribution of glasses can be readily accessed.

2.4. Molecular dynamics simulations

We pick four glasses from the series of experimentally-studied glasses (76 - x)SiO_2–xAl_2O_3–$16Na_2O$–8MgO with x = 0, 8, 16, and 24 for the present simulation study. The model glass samples are made by the following key steps: (1) randomly placing approximately 5000 atoms into a cubic simulation box ($42.3 \times 42.3 \times 42.3$ $Å^3$) and equilibrating them at 4000 K for 4 ns in the *NVT* ensemble to lose the memory of the initial configuration, (2) cooling down the liquid to 3000 K in the *NPT* ensemble for 4 ns under atmospheric pressure to lose the memory of the density of the initial configuration, (3) continuously quenching the melt down to 300 K in the *NPT* ensemble with an average cooling rate of 0.3375 K•ps^{-1}, (4) relaxing the sample under atmospheric pressure for 2 ns. The melt-quenching sample preparation process has been well tested in our previous work [23,40,48,49]. Note that this cooling rate has been found to be low enough to ensure a fair convergence in the structural properties of silicate glasses [37].

We use LAMMPS [50] to run all the simulations and use a timestep of 2 fs. Temperature and pressure are controlled via Nose-Hoover [51,52] thermostat and barostat, respectively. Short-range interactions are described by the well-established Teter [53] potential with a cutoff of 8 Å. The damped shifted force (dsf) method with a cutoff of 10 Å and damping parameter of 0.25 $Å^{-1}$ is used to compute the long-range Columbic interaction [54–58]. The RINGS [59] package is used to conduct basic glass structure analysis, such as neutron total scattering structure factor calculation and ring size distribution analysis. We set the cutoff distance for Si-O bond as

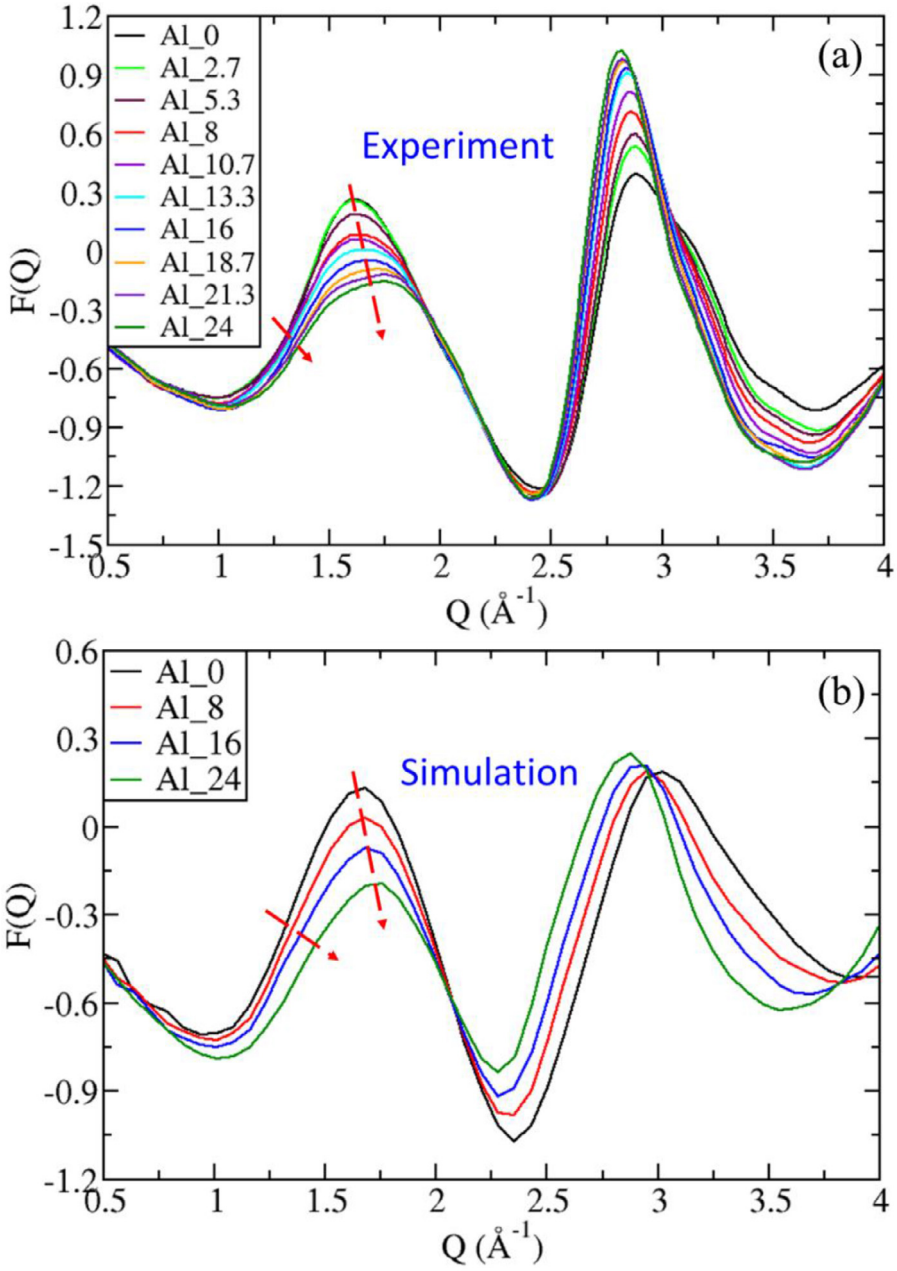

Fig. 1. (a) Experimental neutron total scattering structure factor for the series of MgO sodium aluminosilicate glasses. The spectrum is truncated at $Q = 4$ Å^{-1} to clearly show the characteristics of first sharp diffraction peak revealing the medium-range order structure information. The full spectrums up to $Q = 10$ Å^{-1} are available in Fig. S1 in the Supplementary Material. (b) Corresponding neutron total scattering structure factor from MD simulations for the series of glasses.

1.9 Å, Al-O bond as 2.1 Å, and Mg-O bond as 2.5 Å, for the glass structure analysis. The Ovito [60] software is used to visualize the atomic glass structure.

3. Results

Fig. 1(a) shows the reduced structure factor $F(Q)$ (calculated as $F(Q) = Q(S(Q) - 1)$) measured by neutron total scattering for the series of MgO sodium aluminosilicate glasses. The spectrums are truncated at $Q = 4$ Å^{-1} to highlight the characteristics of the FSDP, which embeds the medium-range structure information of glasses as demonstrated by our latest developed and validated RingFSDP method [45,47]. Interestingly, we can see that the peak position and left shoulder of the FSDP systematically shifts toward high Q direction for the series of glasses with increasing Al_2O_3 content while the right shoulder does not shift accordingly. Based on the RingFSDP analysis, it suggests that the population of large-sized rings continuously gets reduced with increasing Al_2O_3 content (see below for more discussion on this point).

In order to reliably leverage MD simulations to find out the structural role of MgO in this series of glasses, it is crucial to first check whether the simulated glasses also exhibit some FSDP features that are comparable to those observed in experiments. Indeed, it is well known that MD simulations often produce glass structures presenting much higher fictive temperatures than their experimental counterparts due to limited simulations' accessible timescale and, hence, high cooling rates. To this end, Fig. 1(b) shows the corresponding reduced neutron total scattering structure factor $F(Q)$ of four selected MgO sodium aluminosilicate glass samples obtained from MD simulations. Importantly, we observe

that the primary characteristics of the FSDP obtained from experiments are well reproduced in the simulated glass structures, both in terms of peak position and left shoulder shifting—although there remain noticeable differences, which likely arise from the high cooling rate used in MD simulations. For instances, the peak intensity and area of the FSDP (and other peaks) are consistently lower for the simulated glass structures than experimental measurements. Nevertheless, the qualitative agreement of the primary characteristics of FSDP between experiment and simulation demonstrated herein is judged satisfactory enough to lay a solid foundation to further explore the underlying structure role of MgO in this series of glasses.

To assess the network modifier or former nature of Mg^{2+}, we first focus on their coordination number (CN). Indeed, historically, the CN of a cation A has been considered as a key structural feature to discriminate network-forming from -modifying species. For instance, as per Zachariasen rules for glass formation [28], a binary A_mO_n oxide cannot form a glass on its own unless the CN of A is equal to 3 or 4 (note that this condition is necessary, but not sufficient). This empirical rule can be understood from the fact that (i) a CN that is too low does not permit to form an extended 3D network (which is key to kinetically prevent the system from crystalizing), while (ii) a coordination number that is too high does not enable the structural flexibility that is needed to form a disordered (non-crystalline) network.

Fig. 2(a) shows the Mg CN distribution for the series of MgO sodium aluminosilicate glasses. We observe that Mg atoms are predominately four-fold coordinated (Mg^{IV}) for all the samples, which, as per Zachariasen's rules, suggests a network-forming role [28]—in line with previous results from Pedone *et al* [61]. Interestingly, the population of five-fold coordinated Mg atoms (Mg^{V}) increases with increasing content of Al_2O_3, suggesting that some Mg atoms eventually start to act as network modifier/charge compensator in Al-rich glasses. It is also worth mentioning that the Mg coordination will also be largely influenced by the Al_2O_3 content, particularly in alkali-free compositions as clearly demonstrated by Neuville and coworkers [20]. For glasses studied in this work, nearly all the Al atoms are four-fold coordinated due to the significant presence of Na_2O. Additionally, the relatively large population of Mg^{III} for these glasses might be caused by high cooling rate of MD simulations as evidenced in Table S2 in the Supplementary Material.

Network-forming species are also expected to exhibit strong directional bonds, thereby resulting in a well-defined angular environment. To explore the angular environment of Mg atoms, Fig. 2(b) shows the evolution of the O-Mg-O bond angle distribution (BAD) upon increasing Al_2O_3 concentration. As expected, the dominant population of Mg^{IV} atoms lead to the presence of a primary peak angle around 109°. In Al-poor glasses, this peak is initially sharp and well-defined, which further supports the glass former nature of Mg. The increasing population of Mg^{V} upon increasing Al_2O_3 content then results in the emergence of a secondary peak (or shoulder) around 80°. Similarly, the slightly increasing population of Mg^{III} also get manifested as the emergence of a right-shoulder hump at the angle of ~130°, which illustrates that Mg gradually loses its network-forming role upon increasing Al_2O_3 concentration.

Another distinctive feature of network-forming species is their ability to form rings within the atomic networks of glasses—wherein rings are defined as a shortest closed path within the network. In contrast, network-modifying species tend to be connected to terminating non-bridging oxygen (that do not form rings), while charger-compensating species do not explicitly form strong covalent bonds with the rest of the network. To assess whether Mg atoms participate in the formation of rings (together with Si and Al) in the network, we conduct a ring size distribution analysis on the series of glasses considered herein. Out of various ring definitions that are available, we herein adopt the Guttman definition of rings [62] because it produces a realistic total number of rings per network-forming atom (i.e., ~ 6 for fully polymerized glasses) and has proven to be successful in matching results obtained from the experimental RingFSDP method [45]. Fig. 3 shows the ring size distribution for the series of MgO sodium aluminosilicate glasses. The distribution in terms of fraction of each sized ring is available in Fig. S2 in the Supplementary Material. Prior to conducting all the ring statistic calculations, all the Na atoms are dumped from these glasses because they serve as glass network modifiers or charge compensators with Al atoms. To specifically isolate whether or not Mg participates in the formation of rings, we conduct two distinct ring size distribution analyses wherein Mg atoms are (i) initially dumped from the glass structure (solid line) or (ii) kept in the structure (dashed line). The difference between these two distributions specifically captures the population of rings that involve Mg atoms. Clearly, we observe that the computed ring size distribution exhibits a pronounced difference depending on whether or not Mg atoms are initially dumped from the structure. Notably, the total number of rings getting considerably increased when Mg atoms are kept in the glass structure. This highlights the fact that, like Si and Al, Mg atoms do participate in the formation of rings in the glass network. Altogether, these results (i.e., CN, BAD, and ring analysis) show that Mg atoms are part of the backbone of the network structure of aluminosilicate glasses—albeit to a lower extent in Al-rich glasses.

Next, we further investigate what kind of rings (i.e., small or large) are formed by Mg atoms. To this end, Fig. 4 shows the average fraction of Mg atoms per network former (Si, Al, Mg) as a function of ring size for the series of MgO sodium aluminosilicate glasses with increasing Al_2O_3 content considered herein. The fraction of Mg atom per network former in n-membered rings is given by $N_{\text{total number of Mg in the } n\text{−membered ring}}/(n \times N_{\text{number of } n\text{−−membered rings}})$. For all the four samples, we find that Mg atoms predominately reside in the smallest rings, particularly in the three-membered rings. Note that it is technically not appropriate to define a two-membered ring because it simply represents a structure of two edge-sharing tetrahedrons (i.e., that share an edge of two common O atoms), however, it is still interesting to see that Mg atoms are disproportionally represented in this configuration—even through the total population of it is, overall, fairly low (see Fig. 3). Some representative ring configurations are shown in Fig. S3 in the Supplementary Material. Another noticeable observation is that, at fixed ring size, the fraction of Mg atoms systematically decreases upon increasing content of Al_2O_3 (see Fig. 4), which echoes the fact that Mg atoms gradually lose the network-forming role as the Al_2O_3 concentration increases. This can be understood from the fact that, when $[Al_2O_3] > 16\%$, the glass starts to experience a deficit of Na^+ cations—that is, there is not enough Na^+ to charge compensate all the AlO_4 tetrahedral units in the network. As such, from this point, there exists a strong incentive for Mg^{2+} cations to lose their network-forming role so as to turn into charge compensators to stabilize the tetrahedral AlO_4 units. This illustrates the fact that Al and Mg species effectively compete against each other in forming rings—since the need to charge compensate AlO_4 units eventually discourages Mg atoms from participating in the formation of rings in the network.

These results suggest that MgO plays a dual role of glass network modifier/compensator and former, wherein the balance between these two roles depends on composition of the glass. Even though Al competes with Mg to weaken its network-forming role, majority of Mg atoms still participate in the glass network formation (see Figs. 3 and 4). Here, the number of Mg atoms that need to be transformed from network former to charge compensator depends on the balance between the number of Al and Na atoms in

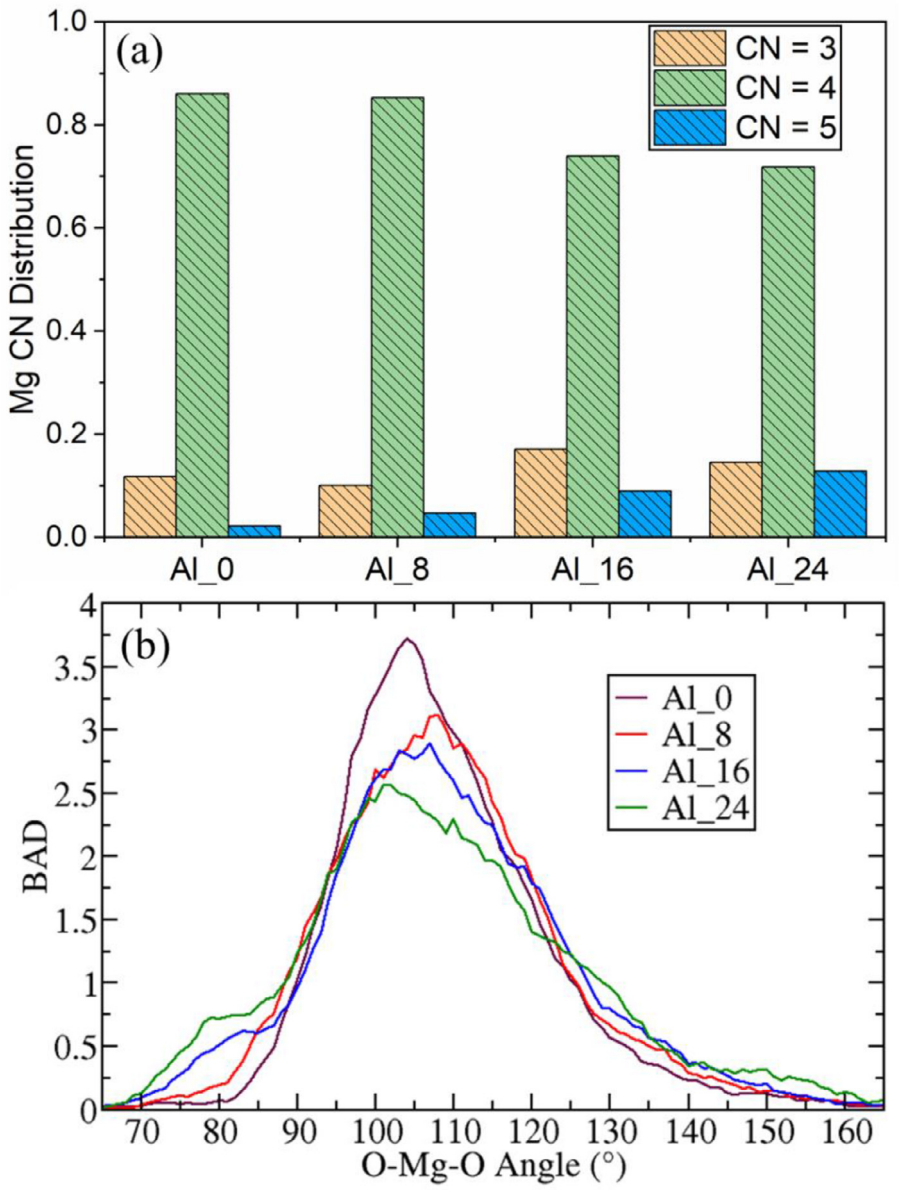

Fig. 2. (a) Distribution of Mg coordination number (CN) in the series of MgO sodium aluminosilicate glasses. (b) The corresponding average O-Mg-O bond angle distribution (BAD) for these glasses.

the glass. When $[Al_2O_3] < [Na_2O]$, all the AlO_4 tetrahedral units can be charge-compensated by available Na^+ cations—so that Mg atoms can act as network formers. In contrast, when $[Al_2O_3] > [Na_2O]$, the number of available Na^+ cations is not large enough to charge compensate all the AlO_4 tetrahedral units—so that a fraction of the Mg need to be "consumed" to charge compensate the excess of AlO_4 tetrahedral units that are not already charge compensated by Na^+ cations. As such, the propensity for Mg atom to act as network former or charge compensator is governed by the balance between (i) the number of Al atoms that need to be charge compensated and (ii) the number of other network modifiers (e.g., Na in the present case) that are available for charge compensation. This mechanism is based on the idea that, whenever possible, AlO_4 units are preferentially charge compensated by Na^+ rather than Mg^{2+} cations. This echoes previous results from Sreenivasan *et al.* [63] demonstrating that, in a series of $(1 - x)Na_2O$–$xMgO$–$0.5Al_2O_3$–$1.25SiO_2$ ($0 \leq x \leq 1$) glasses, Na^+ are preferentially used as charge compensator due to the high field strength of Mg^{2+}.

To further investigate the nature of the competition between Na^+ rather than Mg^{2+} in charge compensating AlO_4 units, we further conduct a series of additional simulations on samples featuring varying levels of Na_2O substitution by MgO (while keeping SiO_2 and Al_2O_3 unchanged). The simulated glass compositions are $(76 - x)SiO_2$–xAl_2O_3–$(24 - y)Na_2O$–$yMgO$ with $x = 0$, 8, 16, 24, and $y = 8$, 16, 24. Fig. 5 shows the population of highly-coordinated Mg atoms (CN $\geq$ 5) as a function of MgO content in the series of MgO sodium aluminosilicate glasses. We observe that this population increases with increasing MgO (i.e., decreasing Na_2O) content for each series of glasses with fixed Al_2O_3 content. In addition, for glasses with fixed MgO content, the population of highly-coordinated Mg atoms also increases with increasing Al_2O_3 content, which is consistent with the observation in Fig. 2. These results confirm that Mg gradually loses its network forming ability (as manifested by the increased fraction of $\geq$ 5-fold coordinated Mg atoms) upon decreasing Na_2O content—since the increasing deficit in Na^+ cations requires Mg^{2+} cations to start acting as charge compensator.

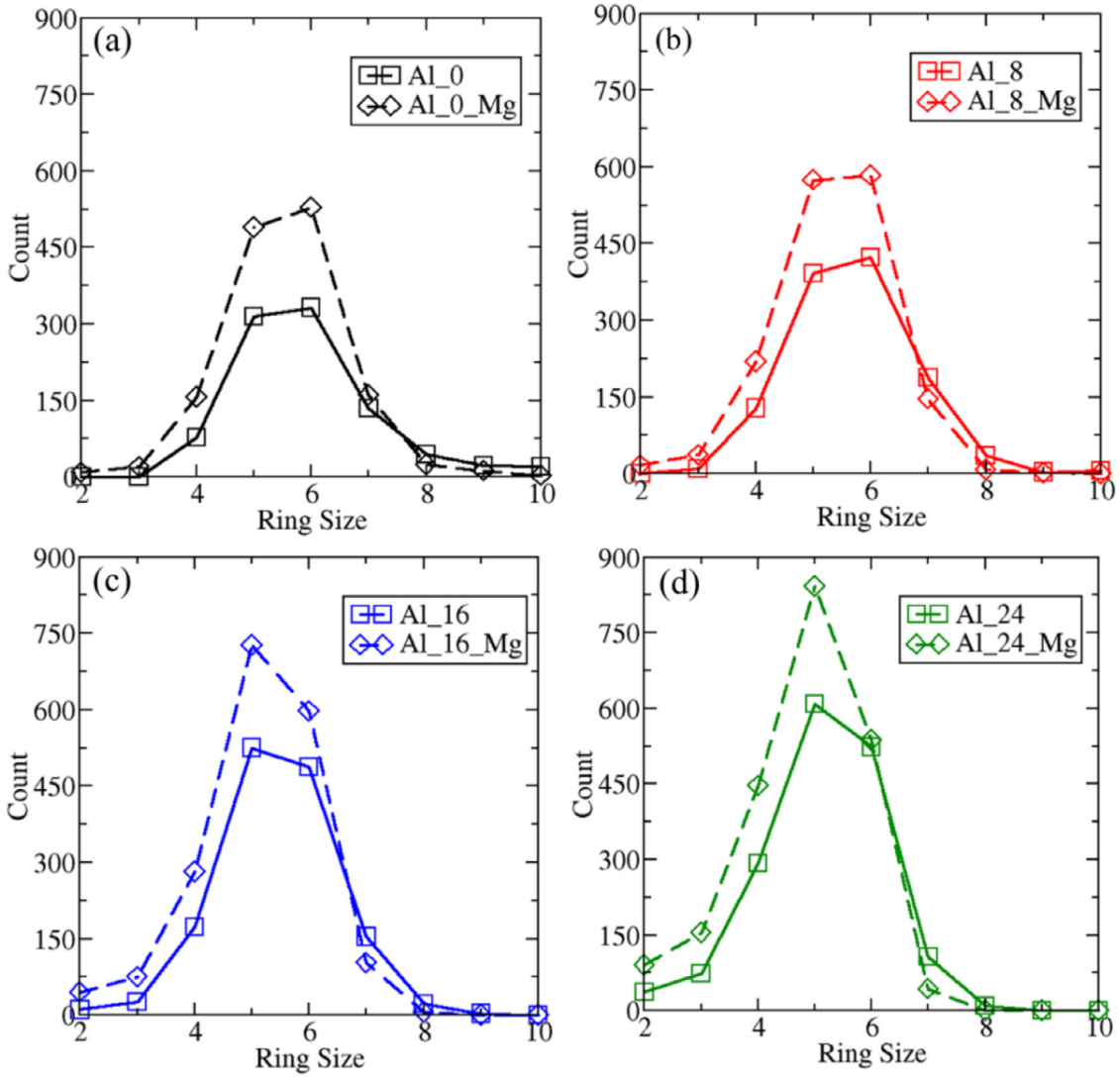

Fig. 3. Gutman ring size distribution for the series of MgO sodium aluminosilicate glasses. All Na atoms are dumped from the glasses before conducting all the ring statistics calculations. Mg atoms are either *dumped from* (solid line) or *kept in* (dash line) the residual glasses for ring statistic calculations to see whether they participate in the formation of rings, e.g. legend 'Al_8' means both Na and Mg atoms are dumped from the glasses, while 'Al_8_Mg' means only Na atoms are dumped from the MgO-containing glasses.

4. Discussions

Having established the structural role of Mg and its ability to form rings in the glass network, we now explore whether this information can be used to decipher the nature of composition-property relationships in MgO sodium aluminosilicate glasses. To this end, we consider the isokom annealing temperature T_{anneal} (i.e., the temperature at which the viscosity is equal to $10^{12.2}$ Pa•s) reported by Smedskjaer *et al.* [32] since this property exhibits a non-linear, non-additive behavior upon increasing Al_2O_3. Specifically, for the series of glasses considered herein, T_{anneal} initially increases fairly linearly with increasing Al_2O_3 content in the [Al_2O3] – [Na_2O] $\leq$ 0 regime, but, notably, exhibits a deviation from linearity (by gradually leveling off) in the [Al_2O3] – [Na_2O] $>$ 0 regime. In the following, we explore whether the structural role of Mg atoms (both in the short- and medium-range order) can explain this deviation from linearity. To this end, three additional samples with Al_2O_3 (mol%) = 4, 12, 20 are simulated to enhance compositional resolution.

We first focus on the short-range order structure. Fig. 6(b) shows the fraction of bridging oxygen (BO) as a function of Al_2O_3 content for the series of glasses. This quantity captures the overall connectivity of the glass, which has been suggested to have a first-order influence on the annealing temperature (as well as on the glass transition temperature) [64]. Note that, here, BOs are defined as oxygen atoms that are connected to two network formers (Si, Al, or Mg)—so that this structural quantity captures the influence of Mg on the glass connectivity. Interestingly, we find that the fraction of BO exhibits a non-linear trend that is similar to that of T_{anneal} with respect to Al_2O_3 content. Specifically, both quantities exhibit the same negative deviation from linearity in the peraluminous regime. This partially arises from the fact Mg atoms lose their network-forming role in the peraluminous regime, which, in turn, reduces the number of BO atoms. This suggests that the glass connectivity indeed plays an influential role in determining the T_{anneal}.

Next, we focus on the medium-range order structure. Fig. 6(c) shows the fraction of small rings ($\leq$ 4) as a function of Al_2O_3 content for the series of simulated glasses considered herein. It should be noted that, here, the computed ring size distribution accounts for the rings created by Mg atoms. Again, we identify a correlation between this trend and that of T_{anneal}. In detail, we observe the existence of a noticeable surge in the population of small-sized

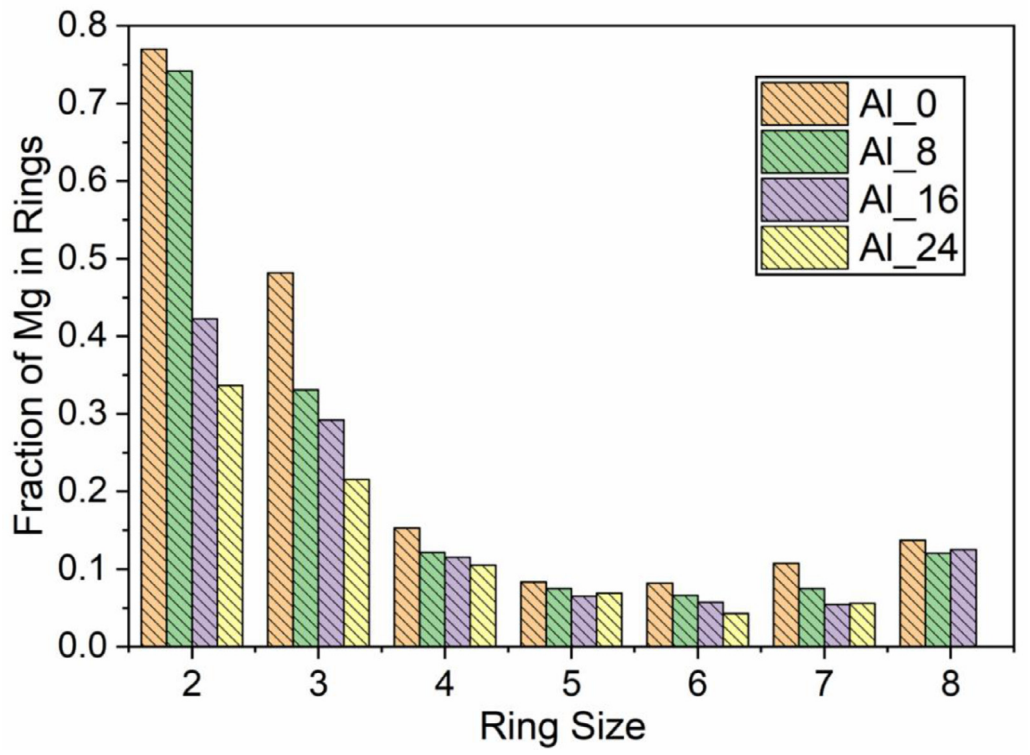

Fig. 4. Average fraction of Mg atoms per network former (Si, Al, Mg) as function of ring size for four MgO sodium aluminosilicate glasses with various Al_2O_3 content.

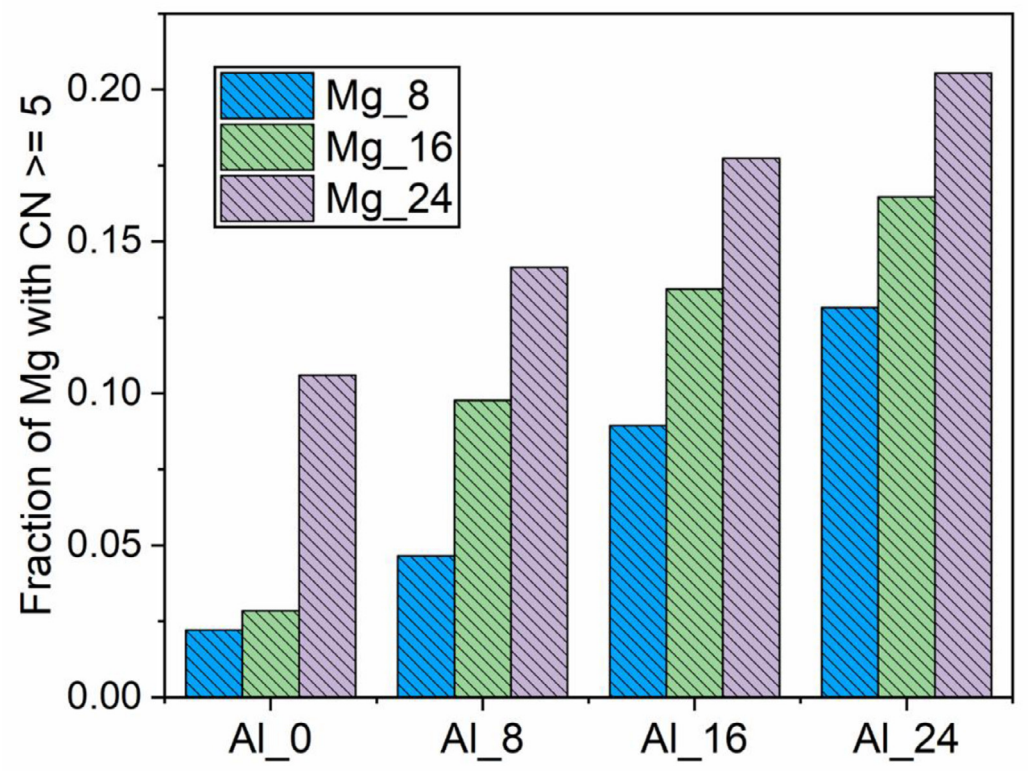

Fig. 5. Population of highly-coordinated Mg atoms (CN $\geq$ 5) as a function of MgO content in the series of MgO sodium aluminosilicate glasses (76 - x)SiO_2–xAl_2O_3–(24 - y)Na_2O–yMgO with x = 0, 8, 16, 24, and y = 8, 16, 24. Note that the population of Mg atoms with CN > 5 is negligible. The ring size distributions for this series of glasses are available in Fig. S4 in the Supplementary Material.

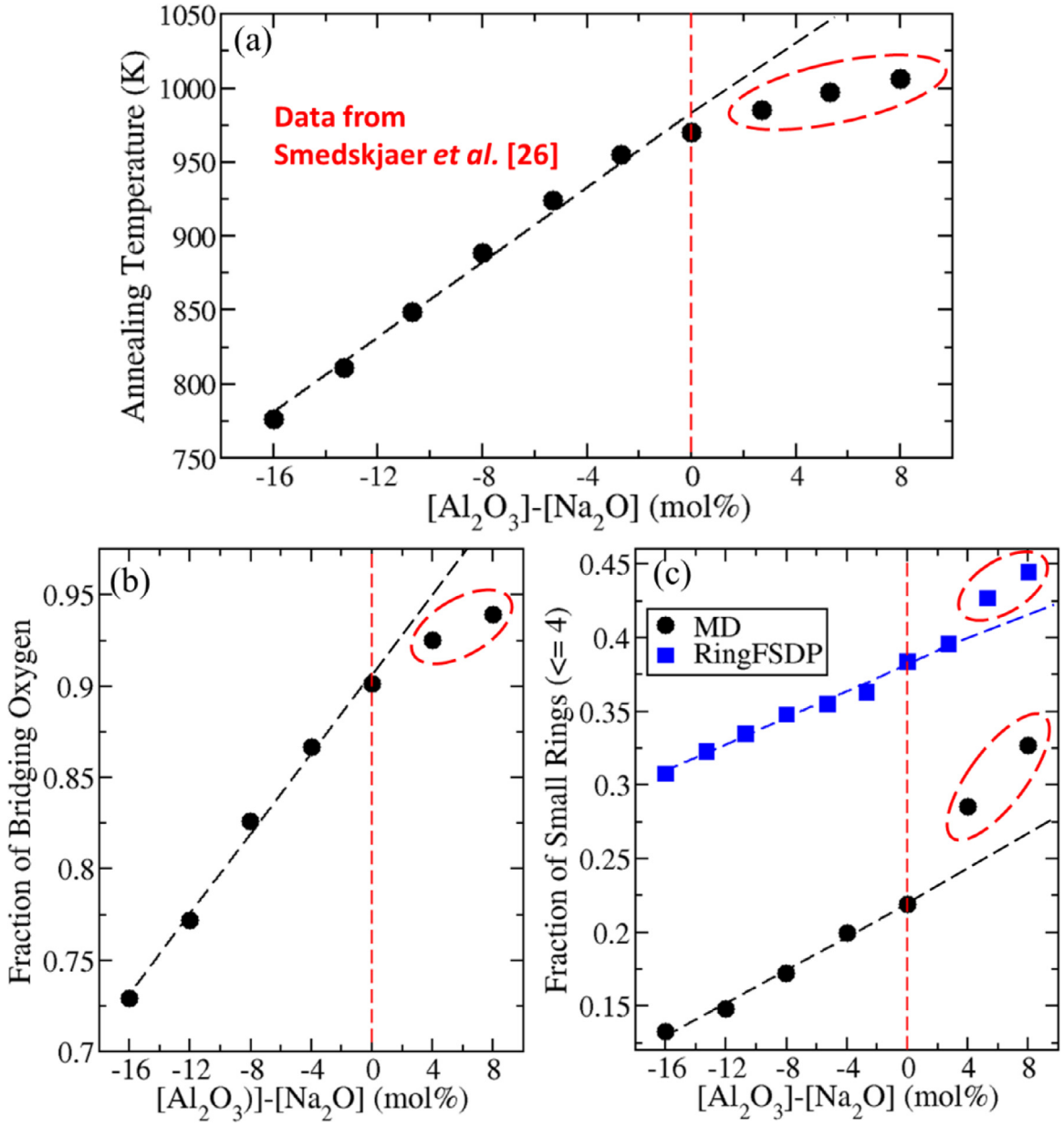

Fig. 6. (a) Composition dependence of the isokom annealing temperature T_{anneal} of the series of MgO sodium aluminosilicate glasses. Data are sourced from a previous study by Smedskjaer *et al.* [32]. T_{anneal} increases fairly linearly with increasing Al_2O_3 content when $[Al_2O3] - [Na_2O] \leq 0$, while it starts to gradually level off when $[Al_2O_3] - [Na_2O] > 0$. (b) Composition dependence of the fraction of bridging oxygen for the series of glasses from MD simulations. (c) Composition dependence of the population of small-sized rings (≤ 4) for MD-synthesized samples (black). Experimental results (blue) offered by the RingFSDP method based on the analysis on the neutron total scattering structure factor as shown in Fig. 1(a) are also shown.

rings (≤ 4) in the $[Al_2O_3] - [Na_2O] > 0$ regime (as indicated by the dashed circle). Note that the spike in the fraction of small-size rings is not simply a consequence of the evolution of the overall connectivity of the glass since, in contrast, the total number of rings keeps increasing linearly as a function of Al_2O_3 content (See Fig. S5 in the Supplementary Material). As a validation of the simulation results, Fig. 6(c) also shows the population of small-sized rings for the 10 experimental samples characterized by our recently developed RingFSDP method *via* deconvolving the FSDP of neutron total scattering structure factors shown in Fig. 1(a). Even though MD simulation underestimates the overall fraction of small rings, we observe an overall harmony between simulation and experimental results—since both present a similar surge in the population of small-sized rings in the peraluminous regime. The description and validation of the RingFSDP approach has been detailed in our previous work [47]. Overall, the concurrent deviation from linearity exhibited by the fraction of small-sized rings and T_{anneal} suggests that, in addition of the short-range connectivity, the medium-range order also influences T_{anneal}. The fact that the annealing temperature levels off as the population of small rings spikes is important since these small rings are specifically those that Mg atoms tend to form (see Fig. 4).

The relationship between annealing temperature and population of small-sized rings can be understood as follows. Conceptually, the isokom T_{anneal} captures how easily a glass deforms under shear stress, wherein a lower T_{anneal} value denotes that the glass shows higher propensity to deform or flow. In that regard, we argue that small-sized rings tend to facilitate the deformation of a glass because they are generally unstable—as suggested by many studies. For instance, Rino *et al.* have shown that small-sized rings

(size = 3 & 4) are energetically unfavorable because they exhibit much higher relative energies as compared to that of 6-membered rings in fused silica [65], which is also suggested by Galeener in the investigation of planner rings in glasses [66]. Song *et al.* have also shown that small-sized rings in sodium silicate glasses exhibit some significant internal stress on account of their overconstrained topological nature, while large-sized rings ($n \geq 6$) do not [38]. Additionally, MD simulations by Yang *et al.* have shown that small-sized rings ($n \leq 4$) exhibit more dramatic change as compared to their larger counterparts for alkaline or alkaline-earth silicate glasses when heated above their respective glass transition temperature [67]. Altogether, this suggests that, in addition to the short-range connectivity, unstable small-sized rings also have a notable influence on annealing temperature. Overall, these results illustrate the important structural role of Mg atoms—since Mg atoms specifically impact both connectivity and the fraction of small-sized rings in the glass.

5. Conclusion

In summary, we carry out extensive studies to investigate the structure role of MgO in sodium aluminosilicate glasses using MD simulations. Detailed analyses on both the short- and medium-range structure strongly suggest that MgO is an intermediate species, not only serving as network modifier/charge compensator, but also participating in the network formation. The competition between these two roles strongly depends on glass composition—and, specifically, on the balance between the number of tetrahedral Al atoms that need to be charge compensated and that of the modifier cations (e.g., Na^+) that are available for charge compensation. Clearly, this conclusion on the modifier versus former role of Mg atoms need to be further confirmed by considering a larger range of glass compositions, as well as other attributes discriminating network modifiers from network formers. Nevertheless, the present results show that explicitly accounting for the structural role played by Mg atoms (both in terms of short-range connectivity and formation of small rings in the medium-range order) is key to understand the relationship between composition and annealing temperature in aluminosilicate glasses. We believe that, more generally, these new findings offer a steppingstone to further decipher the nature of other composition-property relationships in MgO-containing aluminosilicate glasses.

Author contribution

B.D. conceived and conducted the simulations. Y.S. conducted the experimental neutron total scattering measurement. All authors discussed the results and participated in writing and reviewing the paper.

Declaration of Competing Interest

The authors declare that they have no known competing financial interests or personal relationships that could have appeared to influence the work reported in this paper.

Acknowledgements

We are grateful for the technical support from the Corning Scientific Computing group. MB acknowledges funding from the National Science Foundation under grants CMMI-1762292 and DMR-1928538.

Supplementary materials

Supplementary material associated with this article can be found, in the online version, at doi:10.1016/j.actamat.2021.117417.

References

[1] L. Wondraczek, J.C. Mauro, J. Eckert, U. Kuhn, J. Horbach, J. Deubener, T. Rouxel, Towards ultrastrong glasses, Adv. Mater. 23 (39) (2011) 4578–4586.
[2] A. Tandia, K.D. Vargheese, J.C. Mauro, Elasticity of ion stuffing in chemically strengthened glass, J. Non Cryst. Solids 358 (12–13) (2012) 1569–1574.
[3] M. Potuzak, R.C. Welch, J.C. Mauro, Topological origin of stretched exponential relaxation in glass, J. Chem. Phys. 135 (21) (2011) 214502.
[4] M. Potuzak, J.C. Mauro, T.J. Kiczenski, A.J. Ellison, D.C. Allan, Communication: Resolving the vibrational and configurational contributions to thermal expansion in isobaric glass-forming systems, J. Chem. Phys. 133 (9) (2010) 091102.
[5] C.M. Jantzen, K.G. Brown, J.B. Pickett, Durable Glass for Thousands of Years, Int. J. Appl. Glass Sci. 1 (1) (2010) 38–62.
[6] C.M. Jantzen, Systems approach to nuclear waste glass development, J. Non Cryst. Solids 84 (1) (1986) 215–225.
[7] Q. Zheng, M.M. Smedskjaer, R.E. Youngman, M. Potuzak, J.C. Mauro, Y. Yue, Influence of aluminum speciation on the stability of aluminosilicate glasses against crystallization, Appl. Phys. Lett. 101 (4) (2012) 041906.
[8] M.M. Smedskjaer, L. Huang, G. Scannell, J.C. Mauro, Elastic interpretation of the glass transition in aluminosilicate liquids, Phys. Rev. B 85 (14) (2012) 144203.
[9] G.A. Rosales-Sosa, A. Masuno, Y. Higo, H. Inoue, Crack-resistant Al2O3-SiO2 glasses, Sci. Rep. 6 (2016) 23620.
[10] Y. Xiang, J. Du, M.M. Smedskjaer, J.C. Mauro, Structure and properties of sodium aluminosilicate glasses from molecular dynamics simulations, J. Chem. Phys. 139 (4) (2013) 044507.
[11] M.M. Smedskjaer, M. Bauchy, J.C. Mauro, S.J. Rzoska, M. Bockowski, Unique effects of thermal and pressure histories on glass hardness: Structural and topological origin, J. Chem. Phys. 143 (16) (2015) 164505.
[12] S.P. Jaccani, S. Sundararaman, L. Huang, Understanding the structural origin of intermediate glasses, J. Am. Ceram. Soc. (2018).
[13] T.K. Bechgaard, A. Goel, R.E. Youngman, J.C. Mauro, S.J. Rzoska, M. Bockowski, L.R. Jensen, M.M. Smedskjaer, Structure and mechanical properties of compressed sodium aluminosilicate glasses: Role of non-bridging oxygens, J. Non Cryst. Solids 441 (2016) 49–57.
[14] Satoshi Yoshida, Atsuo Hidaka, J. Matsuoka, Crack initiation behavior of sodium aluminosilicate glasses, J. Non Cryst. Solids 344 (2004) 37–43.
[15] J. Kjeldsen, M.M. Smedskjaer, J.C. Mauro, R.E. Youngman, L. Huang, Y. Yue, Mixed alkaline earth effect in sodium aluminosilicate glasses, J. Non Cryst. Solids 369 (2013) 61–68.
[16] K.G. Aakermann, K. Januchta, J.A.L. Pedersen, M.N. Svenson, S.J. Rzoska, M. Bockowski, J.C. Mauro, M. Guerette, L. Huang, M.M. Smedskjaer, Indentation deformation mechanism of isostatically compressed mixed alkali aluminosilicate glasses, J. Non Cryst. Solids 426 (2015) 175–183.
[17] D.R. Neuville, L. Cormier, D. Massiot, Al coordination and speciation in calcium aluminosilicate glasses: Effects of composition determined by 27Al MQ-MAS NMR and Raman spectroscopy, Chem. Geol. 229 (1–3) (2006) 173–185.
[18] J.R. Allwardt, J.F. Stebbins, B.C. Schmidt, D.J. Frost, A.C. Withers, M.M. Hirschmann, Aluminum coordination and the densification of high–pressure aluminosilicate glasses, Am. Mineral. 90 (7) (2005) 1218–1222.
[19] J.F. Stebbins, S. Kroeker, S. Keun Lee, T.J. Kiczenski, Quantification of five- and six-coordinated aluminum ions in aluminosilicate and fluoride-containing glasses by high-field, high-resolution 27Al NMR, J. Non Cryst. Solids 275 (1) (2000) 1–6.
[20] D.R. Neuville, L. Cormier, V. Montouillout, P. Florian, F. Millot, J.C. Rifflet, D. Massiot, Amorphous materials: Properties, structure, and durability: Structure of Mg- and Mg/Ca aluminosilicate glasses: 27Al NMR and Raman spectroscopy investigations, Am. Mineral. 93 (11–12) (2008) 1721–1731.
[21] M. Ren, J.Y. Cheng, S.P. Jaccani, S. Kapoor, R.E. Youngman, L. Huang, J. Du, A. Goel, Composition – structure – property relationships in alkali aluminosilicate glasses: A combined experimental – computational approach towards designing functional glasses, J. Non Cryst. Solids 505 (2019) 144–153.
[22] L. Deng, S. Urata, Y. Takimoto, T. Miyajima, S.H. Hahn, A.C.T. Duin, J. Du, Structural features of sodium silicate glasses from reactive force field-based molecular dynamics simulations, J. Am. Ceram. Soc. 103 (3) (2019) 1600–1614.
[23] B. Deng, A. Tandia, Y. Shi, Impact of pressure on structure and properties of hot-compressed Na2O–Al2O3–SiO2 glass by molecular dynamics simulations, J. Am. Ceram. Soc. 104 (6) (2021) 2530–2538.
[24] H. Liu, B. Deng, S. Sundararaman, Y. Shi, L. Huang, Understanding the response of aluminosilicate and aluminoborate glasses to sharp contact loading using molecular dynamics simulation, J. Appl. Phys. 128 (3) (2020).
[25] A. Zeidler, P.S. Salmon, L.B. Skinner, Packing and the structural transformations in liquid and amorphous oxides from ambient to extreme conditions, Proc. Natl. Acad. Sci. U. S. A. 111 (28) (2014) 10045–10048.
[26] L. Cormier, G.J. Cuello, Structural investigation of glasses along the MgSiO3–CaSiO3 join: Diffraction studies, Geochim. Cosmochim. Acta 122 (2013) 498–510.
[27] M.M. Smedskjaer, R.E. Youngman, J.C. Mauro, Impact of ZnO on the structure and properties of sodium aluminosilicate glasses: Comparison with alkaline earth oxides, J. Non Cryst. Solids 381 (2013) 58–64.
[28] W.H. Zachariasen, THE ATOMIC ARRANGEMENT IN GLASS, J. Am. Chem. Soc. 54 (10) (1932) 3841–3851.
[29] K.-H. Sun, Fundamental condition of glass formation, J. Am. Ceram. Soc. 30 (9) (1947) 277–281.
[30] A. Dietzel, Strukturchemie des Glases, Naturwissenschaften 29 (36) (1941) 537–547.
[31] M. Lograd, H. Eckert, T. Murata, S. Nakane, H. Yamazaki, Structure-property

relations in crack-resistant alkaline-earth aluminoborosilicate glasses studied by solid state NMR, J. Am. Ceram. Soc. 104 (5) (2021) 2250–2267.
[32] M.M. Smedskjaer, J.C. Mauro, J. Kjeldsen, Y. Yue, T. Rouxel, Microscopic Origins of Compositional Trends in Aluminosilicate Glass Properties, J. Am. Ceram. Soc. 96 (5) (2013) 1436–1443.
[33] S.K. Lee, H.-I. Kim, E.J. Kim, K.Y. Mun, S. Ryu, Extent of Disorder in Magnesium Aluminosilicate Glasses: Insights from27Al and17O NMR, J. Phys. Chem. C 120 (1) (2015) 737–749.
[34] T.K. Bechgaard, G. Scannell, L. Huang, R.E. Youngman, J.C. Mauro, M.M. Smedskjaer, Structure of MgO/CaO sodium aluminosilicate glasses: Raman spectroscopy study, J. Non Cryst. Solids 470 (2017) 145–151.
[35] M.T. Souza, M.C. Crovace, C. Schröder, H. Eckert, O. Peitl, E.D. Zanotto, Effect of magnesium ion incorporation on the thermal stability, dissolution behavior and bioactivity in Bioglass-derived glasses, J. Non Cryst. Solids 382 (2013) 57–65.
[36] M. Guignard, L. Cormier, Environments of Mg and Al in MgO–Al2O3–SiO2 glasses: A study coupling neutron and X-ray diffraction and Reverse Monte Carlo modeling, Chem. Geol. 256 (3) (2008) 111–118.
[37] X. Li, W. Song, K. Yang, N.M.A. Krishnan, B. Wang, M.M. Smedskjaer, J.C. Mauro, G. Sant, M. Balonis, M. Bauchy, Cooling rate effects in sodium silicate glasses: Bridging the gap between molecular dynamics simulations and experiments, J. Chem. Phys. 147 (7) (2017) 074501.
[38] Weiying Song, Xin Li, Bu Wang, John C. Mauro, N.M. Anoop Krishnan, Sushmit Goyal, Morten M. Smedskjaer, Christian G. Hoover, M. Bauchy, Atomic picture of structural relaxation in silicate glasses, Appl. Phys. Lett. 114 (2019) 233703.
[39] Y.T. Shih, S. Sundararaman, L. Huang, Structural origin of the anomalous density maximum in silica and alkali silicate glasses, J. Am. Ceram. Soc. (2019).
[40] B. Deng, Y. Shi, F. Yuan, Investigation on the structural origin of low thermal expansion coefficient of fused silica, Materialia 12 (2020).
[41] Y. Yang, O. Homma, S. Urata, M. Ono, J.C. Mauro, Topological pruning enables ultra-low Rayleigh scattering in pressure-quenched silica glass, npj Comput. Mater. 6 (1) (2020).
[42] Y. Yang, H. Tokunaga, K. Hayashi, M. Ono, J.C. Mauro, Understanding thermal expansion of pressurized silica glass using topological pruning of ring structures, J. Am. Ceram. Soc. (2020).
[43] M.M. Smedskjaer, S.A. Saxton, A.J. Ellison, J.C. Mauro, Photoelastic response of alkaline earth aluminosilicate glasses, Opt. Lett. 37 (3) (2012) 293–295.
[44] J. Neuefeind, M. Feygenson, J. Carruth, R. Hoffmann, K.K. Chipley, The Nanoscale Ordered MAterials Diffractometer NOMAD at the Spallation Neutron Source SNS, Nuclear Instruments and Methods in Physics Research Section B: Beam Interactions with, Mater. Atoms 287 (2012) 68–75.
[45] Y. Shi, J. Neuefeind, D. Ma, K. Page, L.A. Lamberson, N.J. Smith, A. Tandia, A.P. Song, Ring size distribution in silicate glasses revealed by neutron scattering first sharp diffraction peak analysis, J. Non Cryst. Solids 516 (2019) 71–81.
[46] Y. Shi, N.T. Lonnroth, R.E. Youngman, S.J. Rzoska, M. Bockowski, M.M. Smedskjaer, Pressure-induced structural changes in titanophosphate glasses studied by neutron and X-ray total scattering analyses, J. Non Cryst. Solids 483 (2018) 50–59.
[47] Q. Zhou, Y. Shi, B. Deng, J. Neuefeind, M. Bauchy, Experimental method to quantify the ring size distribution in silicate glasses and simulation validation thereof, Sci. Adv. 7 (28) (2021) eabh1761.
[48] B. Deng, J. Luo, J.T. Harris, C.M. Smith, T.M. Wilkinson, Toward revealing full atomic picture of nanoindentation deformation mechanisms in Li2O-2SiO2 glass-ceramics, Acta Mater. 208 (2021).
[49] M.E. McKenzie, B. Deng, D.C. Van Hoesen, X. Xia, D.E. Baker, A. Rezikyan, R.E. Youngman, K.F. Kelton, Nucleation pathways in barium silicate glasses, Sci. Rep. 11 (1) (2021) 69.
[50] S. Plimpton, Fast Parallel Algorithms for Short-Range Molecular Dynamics, J. Comput. Phys. 117 (1) (1995) 1–19.
[51] S. Nosé, A unified formulation of the constant temperature molecular dynamics methods, J. Chem. Phys. 81 (1) (1984) 511–519.
[52] W.G. Hoover, Canonical dynamics: Equilibrium phase-space distributions, Phys. Rev. A 31 (3) (1985) 1695–1697.
[53] J. Du, Challenges in Molecular Dynamics Simulations of Multicomponent Oxide Glasses, in: C. Massobrio, J. Du, M. Bernasconi, P.S. Salmon (Eds.), Molecular Dynamics Simulations of Disordered Materials: From Network Glasses to Phase-Change Memory Alloys, Springer International Publishing, Cham, 2015, pp. 157–180.
[54] B. Deng, J.T. Harris, J. Luo, Atomic picture of crack propagation in Li2O-2SiO2 glass-ceramics revealed by molecular dynamics simulations, J. Am. Ceram. Soc. 103 (8) (2020) 4304–4312.
[55] J. Luo, K.D. Vargheese, A. Tandia, J.T. Harris, J.C. Mauro, Structural origin of intrinsic ductility in binary aluminosilicate glasses, J. Non Cryst. Solids 452 (2016) 297–306.
[56] B. Deng, J. Luo, J.T. Harris, C.M. Smith, M.E. McKenzie, Molecular dynamics simulations on fracture toughness of Al2O3-SiO2 glass-ceramics, Scr. Mater. 162 (2019) 277–280.
[57] B. Deng, J. Luo, J.T. Harris, C.M. Smith, Critical stress map for ZrO2 tetragonal to monoclinic phase transformation in ZrO2-toughened glass-ceramics, Materialia 9 (2020).
[58] B. Deng, J.T. Harris, A novel approach to generate glass-ceramics samples for molecular dynamics simulations, Comput. Mater. Sci. 186 (2021).
[59] S.Le Roux, P. Jund, Ring statistics analysis of topological networks: New approach and application to amorphous GeS2 and SiO2 systems, Comput. Mater. Sci. 49 (1) (2010) 70–83.
[60] S. Alexander, Visualization and analysis of atomistic simulation data with OVITO–the Open Visualization Tool, Model. Simul. Mater. Sci. Eng. 18 (1) (2010) 015012.
[61] A. Pedone, G. Malavasi, M.C. Menziani, U. Segre, A.N. Cormack, Role of Magnesium in Soda-Lime Glasses: Insight into Structural, Transport, and Mechanical Properties through Computer Simulations, J. Phys. Chem. C 112 (29) (2008) 11034–11041.
[62] L. Guttman, Ring structure of the crystalline and amorphous forms of silicon dioxide, J. Non Cryst. Solids 116 (2) (1990) 145–147.
[63] H. Sreenivasan, P. Kinnunen, E. Adesanya, M. Patanen, A.M. Kantola, V.-V. Telkki, M. Huttula, W. Cao, J.L. Provis, M. Illikainen, Field Strength of Network-Modifying Cation Dictates the Structure of (Na-Mg) Aluminosilicate Glasses, Front. Mater. 7 (2020).
[64] M. Micoulaut, Glass Transition Temperature Variation as a Probe for Network Connectivity, in: M.F. Thorpe, J.C. Phillips (Eds.), Phase Transitions and Self-Organization in Electronic and Molecular Networks, Springer US, Boston, MA, 2001, pp. 143–160.
[65] J.P. Rino, I. Ebbsjö, R.K. Kalia, A. Nakano, P. Vashishta, Structure of rings in vitreous SiO2, Phys. Rev. B 47 (6) (1993) 3053–3062.
[66] F.L. Galeener, Planar rings in glasses, Solid State Commun. 44 (7) (1982) 1037–1040.
[67] Y. Yang, H. Tokunaga, M. Ono, K. Hayashi, J.C. Mauro, Thermal expansion of silicate glass-forming systems at high temperatures from topological pruning of ring structures, J. Am. Ceram. Soc. 103 (8) (2020) 4256–4265.